

# Structural Characterization of Stoichiometric Calcium Hydroxyapatite Prepared from Aqueous Solution at Room Temperature and Neutral pH

B. El ouatli, F. Abida, A. Elouahli, M. Jamil, M. Ezzahmouly, H. Khallok, Z. Hatim  
Team of Electrochemistry and Biomaterials, Department of Chemistry, Faculty of Sciences,  
University of Chouaib Doukkali, El Jadida, Morocco.

**Abstract**— In this study structural characterization of stoichiometric calcium hydroxyapatite ( $\text{Ca}_{10}(\text{PO}_4)_6(\text{OH})_2$ ) powder is investigated. The sample was prepared from aqueous solutions, under air atmosphere at 22°C and neutral pH. The powder calcined at 1100°C was investigated by chemical characterization, thermal analysis and X-ray pattern fitting methods. Results showed that hydroxyapatite can successfully be produced at room temperature and neutral pH without other calcium phosphate impurities. Trace ions as  $\text{Na}^+$ ,  $\text{Mg}^{2+}$ ,  $\text{Sr}^{2+}$ ,  $\text{SO}_4^{2-}$ , and  $\text{CO}_3^{2-}$  were detected and coupled substitution of cation and anion trace affects neither the theoretical structure nor the thermal stability of the hydroxyapatite but creates vacancies in calcium (Ca1) and oxygen (O1 and O3) sites. This structural change leads to a slight lattice distortion ( $D_{\text{ind}} = 3.204$ ) compared to the theoretical value ( $D_{\text{ind}} = 3.079$ ). The structure showed the dehydroxylation between 950°C and 1300°C and the decomposition, into both tri-calcium phosphate ( $\text{Ca}_3(\text{PO}_4)_2$ ) and tetra-calcium phosphate ( $\text{Ca}_4(\text{PO}_4)_2\text{O}$ ), takes place at 1450 °C.

**Index Terms**— Calcium-Hydroxyapatite, Stoichiometry, Ions trace, Crystalline Structure.

## 1 INTRODUCTION

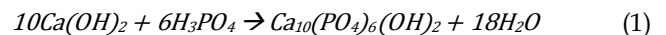
IN recent years, significant research effort has been devoted to developing powder of hydroxyapatite ( $\text{Ca}_{10}(\text{PO}_4)_6(\text{OH})_2$ , HAP) because of its potential application in many interdisciplinary fields including chemistry, biology and medicine [1],[2],[3]. The prepared hydroxyapatite, due to its identical structure of the natural bone, has good compatibility with the human organism, and is widely used in medical applications as an implant or as a coating on prosthesis [4],[5],[6]. Calcium-hydroxyapatite is used in the form of powder, granule, block or the injectable paste, its uses requiring shaping and treatment at high temperature [7],[8],[9]. Several techniques have been used for HAP powders preparation (wet synthesis, solid-state reaction and hydrothermal methods etc) [10],[11],[12] and materials with various composition, stoichiometry, and crystallinity, have been obtained. These properties affect the physical and chemical properties, such as shaping of powder, thermal stability, bioactivity and dissolution behavior [13],[14],[15].

Stoichiometric hydroxyapatite is generally prepared in aqueous solutions by mixing exactly stoichiometric quantities of  $\text{Ca}^{2+}$  and  $\text{PO}_4^{3-}$  containing solutions at  $\text{pH} > 9$ , followed by

boiling for several days in  $\text{CO}_3^{2-}$  free atmosphere (the ageing or maturation stage), the Ca/P molar ratio of 1,667 was found

to be attained after the completion of the reaction at 90°C [16],[17]. The main difficulty encountered in the production of hydroxyapatite is the formation of non-stoichiometric products [18] due to the experimental conditions in particular the temperature, the pH and the contamination by the reagents used, including sodium, potassium, chloride and nitrate, showing a strong affinity for hydroxyapatite.

In our laboratory we are interested in the preparation, under industrial conditions, of stoichiometric hydroxyapatite powder with a controlled chemical composition and crystallographic structure. The powders are prepared from supersaturated aqueous solutions following the chemical reaction:



This non-polluting method appears to be very promising for the preparation of hydroxyapatite powders in industrial scale. The stoichiometry and structural properties of produced hydroxyapatite are influenced by the purity of the raw materials [19] and by operating parameters such as the flow rate of reagent, stirring rate, pH and temperature [20].

The materials generated will have a different profile of thermal stability, bioactivity and dissolution behaviour. The aim of the present work is the control of the structural atomic rearrangement in stoichiometric hydroxyapatite prepared by

• Corresponding author: M. Jamil  
E-mail: mo.jamil@yahoo.fr

the reaction between calcium hydroxide and orthophosphoric acid, under air atmosphere at room temperature and neutral pH. The prepared powder was investigated by chemical characterization, thermal analysis and X-ray powder pattern fitting methods with the means of program FULLPROF WINPLOTR 2012. Crystallographic data available in database will be designated as theoretical values.

## 2 MATERIALS AND METHODS

### 2.1 powders preparation

500g of calcium-hydroxyapatite powders were synthesized by reaction between the calcium hydroxide and orthophosphoric acid under air atmosphere. The flowchart for the synthesis of the hydroxyapatite is illustrated in Fig. 1. The first time, CaCO<sub>3</sub> (analytical grade) was heated at 900°C over 12 hours. The obtained CaO powder was hydrated with double distilled water to produce Ca(OH)<sub>2</sub> (0,6 mol/l). The appropriate amount of orthophosphoric acid (analytical grade) solution (1mol/l) was added into Ca(OH)<sub>2</sub> suspension using an automatic titration (100 ml/min) and vigorous stirring (500T/min). The calcium / phosphorus molar ratio of the reagents is fixed at 1.667 (molar ratio of the stoichiometric hydroxyapatite). The reaction mixture is carried out at 22°C and the pH precipitation is from 7.5. The resulting precipitate was aged for 12 h decanted then filtered, dried at 105°C for 24 hours and calcined at 1100°C for 10 hours.

### 2.2 Characterization of powders

#### 2.2.1 Chemical characterization

The prepared powder was identified by means of the atomic ratios Ca/P using the infrared spectroscopy (PerkinElmer FTIR 1600), and X-ray diffraction (Siemens 5000). Chemical tests were performed to detect traces of lime (CaO). The chemical analysis was determined by atomic emission spectrophotometer, argon plasma and inductive coupling (ICPAES) (ThermoJarrel Ash. Atom Scan 16). Carbonate content is determined by HCN analysis.

#### 2.2.2 Thermal analysis

Thermal Analysis was performed on Netzsch STA 429 facility with a conventional PtPt/Rh sample holder capable of simultaneous recording of thermogravimetric (TG) and differential thermal analysis (DTG) curves in the temperature range of 20 to 1450°C. The measurements of the powder sample (30 mg) were recorded under ambient pressure and at a heating rate of 10°C/min.

#### 2.2.3 Structural refinement

The X-ray powder data were collected on D5000 operating in step scan mode using Cu radiation. X-ray data were collected with a 0.02° 2θ step and counting 15s by step.

FullProf codes [21] were used to perform Rietveld refinements. Refined values (a and c cell parameters, atomic positions, site occupancies, thermal parameters) of stoichiometric hydroxyapatite [22] were used as the starting model. The pseudo-Voigt function was used to present the individual reflection profiles. In the final step of the refinement, all atomic positions and site occupancies were refined simultaneously with atom displacement factor. In the last cycle of refinement, 33 structural and non-structural parameters were optimized.

The distortion of the structure can be calculated from the tetrahedron PO<sub>4</sub> according to the Eqs (1) [23]. D<sub>ind</sub> represents the deviation of the tetrahedron PO<sub>4</sub> in the structure and terms θ represents OPO angle.

$$D_{ind} = \frac{\sum_{i=1}^{i=6} (\theta_i - 109.17)^2}{6} \quad (2)$$

From the refinement, the Rc hydroxyl channel radius is calculated using Eqs (2).

$$R_c = \frac{d(Ca_2 - Ca_2)}{2} \operatorname{tg} \frac{\pi}{6} \quad (3)$$

d(Ca2-Ca2) stands for a bond length.

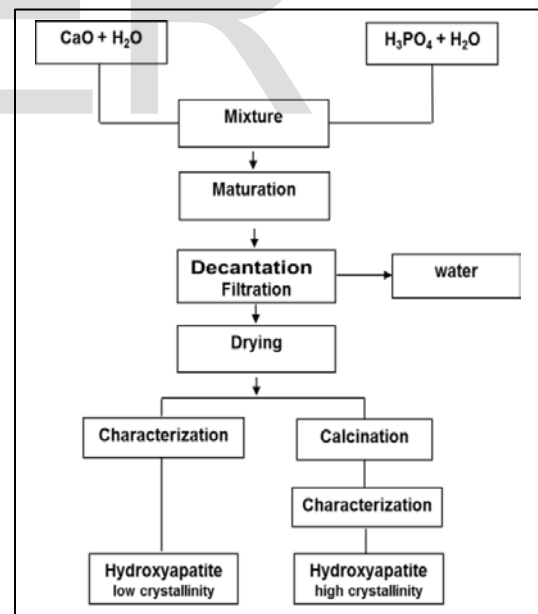


Fig.1: Flowchart for the synthesis of the Hydroxyapatite

## 3 RESULTS

### 3.1. Powder characterization

#### 3.1.1 Chemical analysis

The chemical analysis of calcium and phosphor concentration listed in Table 1, was carried out on the calcined sample and the results was compared to available data designated, in this work, as theoretical values ( $HAP_{THE}$ ). The considered trace ions ( $Na^+$ ,  $Mg^{2+}$ ,  $Sr^{2+}$ ,  $SO_4^{2-}$ ) concentrations are also listed in this Table. Other elements such as Aluminium, Fer and Zinc are present in weight proportions of less than 10 ppm. Total mass fraction of the trace elements was estimated to 612 ppm for the prepared HAP powder. We can specify that  $Mg^{2+}$  and  $Sr^{2+}$  ions are brought by the calcium carbonate while the  $Na^+$  and  $SO_4^{2-}$  ions are brought by orthophosphorique acid and calcium carbonate.

The sample was precipitated at room temperature at pH from 7.5 under air atmosphere which leads to contamination of product by air carbonate. The carbonate ions ( $CO_3^{2-}$ ) are detected in prepared hydroxyapatite with concentration from 0.46 wt %.

### 3.1.2 Infrared spectroscopy and gravimetric analysis

The infrared spectre of calcined powder, reported in Fig 2(a), shows on the one hand the presence of only one well-crystallized phase of the hydroxyapatite, and, on the other hand the absence of carbonate and other calcium phosphates such as tri-calcium phosphates or calcium oxide.

We can specify that the infrared spectrum of the dried powder to 105°C (fig 2(b) shows the low crystallinity of hydroxyapatite and the presence of the bands corresponding to carbonates grouping ( $CO_3^{2-}$ ).

Thermogravimetric curve of prepared hydroxyapatite is reported in Fig 3. The sample loses its weight quickly when the temperature is less than 400°C; the weight loss between 950°C to 1300°C is associated with a large endothermic effect. At 1450°C, the weight loss accelerated strongly and an inflection can be observed.

### 3.1.3 X-ray diffraction patters and Rietveld refinement

The Pattern from X-ray diffraction for prepared HAP is displayed in Fig 4. This shows the high crystallinity and the purity of the synthetic hydroxyapatite phase calcined at 1100°C and no influence of trace ions is evidenced.

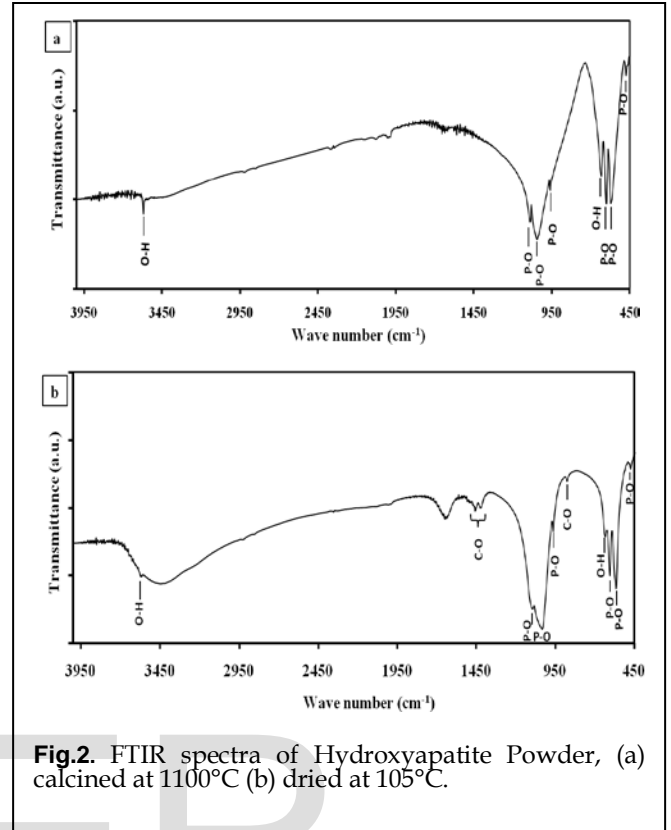


Fig.2. FTIR spectra of Hydroxyapatite Powder, (a) calcined at 1100°C (b) dried at 105°C.

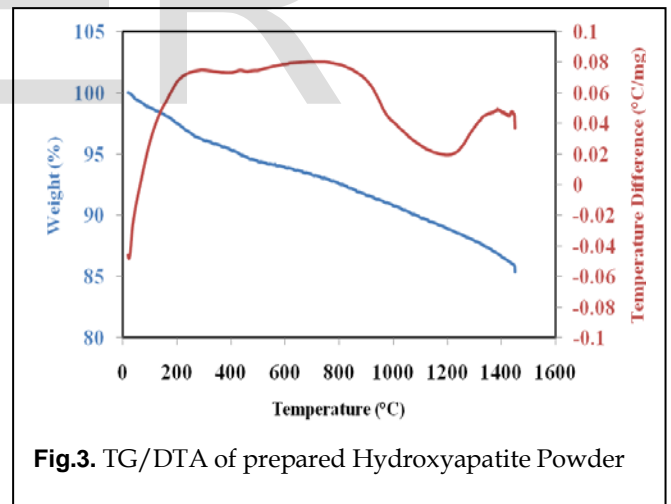


Fig.3. TG/DTA of prepared Hydroxyapatite Powder

Table1: Chemical composition of prepared and theoretical Hydroxyapatite

Sample	Ca (%)	P (%)	Ca/P (Molar ratio)	$CO_3^{2-}$ (%)	$Mg^{2+}$ (ppm)	$Na^+$ (ppm)	$Sr^{2+}$ (ppm)	$S^{2-}$ (ppm)
HAP	38,87 ± 0,54	18,05 ± 0,22	1,664 ± 0,005	0,46	111	179	119	203
$HAP_{THE}$	39,90	18,50	1,666	-	-	-	-	-

Rietveld refinement is expected to give more detailed information about structural atomic rearrangement and trace ions incorporation in the stoichiometric hydroxyapatite. According to the Rietveld method with the means of program FULLPROF WINPLOTR 2012 [21], the structure refinement was performed. The structure of prepared sample was refined considering, as a starting point, the model of theoretical hydroxyapatite (HAP<sub>THE</sub>) for which we used parameters reported by Sandarsanan and Young [22]. Cell parameters are determined and compared to theoretical values (Table 2). Parameters as  $D_{ind}$  distortion index,  $R_c$  values and volume are gathered in Table 3 and compared to the theoretical values as well. In addition, atom coordinates were refined and listed in Table 5. So, the prepared hydroxyapatite crystallized in hexagonal system with unit cell parameters reported in Table 2. Cell parameters ( $a = b = 9.408 \text{ \AA}$ ,  $c = 6.872 \text{ \AA}$ ) are slightly lower than those found in theory ( $a = b = 9.419 \text{ \AA}$ ,  $c = 6.88 \text{ \AA}$ ).

The result of the structural refinement shows that the perturbation in the P-O distance is marked and distances between calcium and oxygen atoms present a disturbance (Table 4): we can notice P-O2 distances decrease; while P-O1 and P-O3 distances increase. Ca2-O2 distances increase; while Ca1-O1 and Ca2-O3 distances decrease. The Phosphorus and calcium occupancy rate, given in Table 5, is slightly less than the theoretical value while the oxygen (O1, O2 and O3) occupancy rate is slightly greater than the theoretical value given in table 6. The B factor value is lower than 1 for Ca2, P and O2 atoms, and exceed 1 for Ca1, O1 and O3 atoms and a slight displacements of the OH atoms position is observed. The ion position shifts from  $z = 0,198$  in theoretical HAP (Table 6) to  $z = 0.196$  (Table 6). The volume of the cell ( $526.74 \text{ \AA}^3$ ) is also slightly below the theoretical value ( $529.16 \text{ \AA}^3$ ) and the  $D_{ind}$  distortion index ( $D_{ind} = 3.204$ ) is slightly larger as that calculated for the theoretical value ( $D_{ind} = 3.079$ ) (Table 3).

#### 4. DISCUSSION

The IR spectroscopy, X-ray diffraction pattern and the chemical test result show that the prepared powder can be considered as pure hydroxyapatite.

Chemical analysis of calcined sample reveals the presence of trace ions as  $\text{Na}^+$ ,  $\text{Mg}^{2+}$ ,  $\text{Sr}^{2+}$  and  $\text{SO}_4^{2-}$ , with total sum estimated to 612 ppm and 0.46 % for carbonate ( $\text{CO}_3^{2-}$ ) mass fraction. Calculated  $\text{Ca/P} = 1.664 \pm 0.005$  molar ratio is close to the theoretical values whereas the calcium and phosphorus mass fractions are slightly lower than the values found for the stoichiometric hydroxyapatite. These results reveal the presence of calcium vacant sites and/or the substitution of calcium and phosphorus by trace ions but these slight modifications did not seem to affect the theoretical structure of prepared hydroxyapatite.

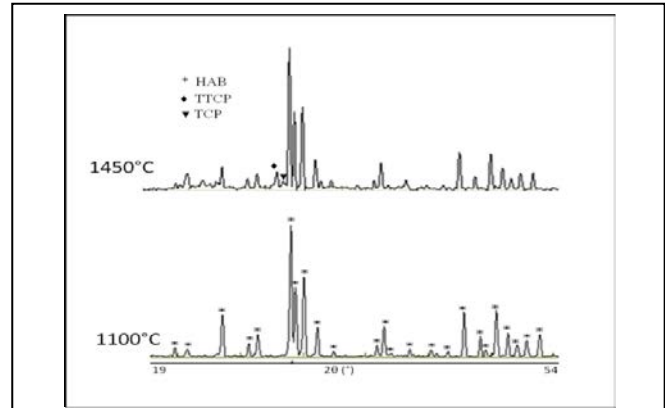


**Fig.4:** X-ray Diffraction Patterns of calcined Hydroxyapatite Powder at 1100°C and 1450°C.

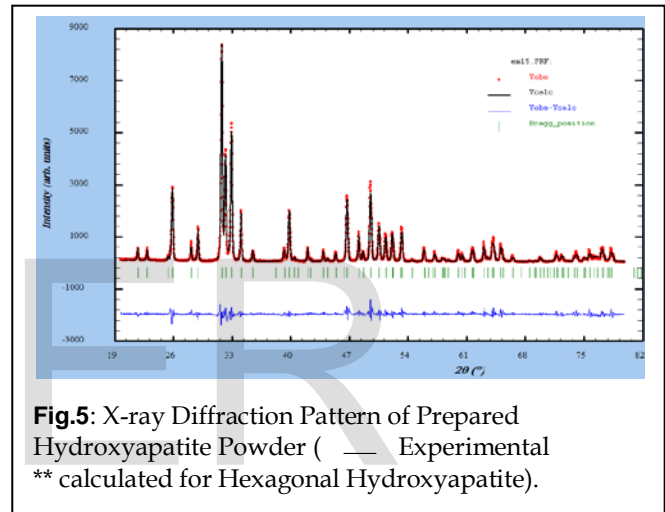


**Fig.5:** X-ray Diffraction Pattern of Prepared Hydroxyapatite Powder ( — Experimental \*\* calculated for Hexagonal Hydroxyapatite).

**Table 2:** Calculated cell parameters of prepared and theoretical Hydroxyapatite

sample	HAP	HAP <sub>THE</sub>
a (Å)=b (Å)	9.408	9.419
c (Å)	6.872	6.88
$\alpha(^{\circ})=\beta(^{\circ})$	90.000	90.000
$\gamma(^{\circ})$	120.000	120.000
Groupe spatial	P 63/m	P 63/m

**Table 3:** Distortion index ( $D_{ind}$ ), volume and  $R_c$  values of prepared and theoretical Hydroxyapatite

Sample	HAP	HAP <sub>THE</sub>
$D_{ind}$	3.204	3.079
$R_c$ (Å)	1.178	1.177
V (Å <sup>3</sup> )	526.74	529.16

According to the reported work [24], an apatitic lattice always contains 6 groups of  $\text{PO}_4^{3-}$  with the possible substitutions such as  $\text{SiO}_4^{4-}$ ,  $\text{CO}_3^{2-}$  and  $\text{SO}_4^{2-}$ ... Based on our chemical analysis, the  $\text{CO}_3^{2-}$  and  $\text{SO}_4^{2-}$  presence are confirmed (Table 1).



Partial replacement of  $\text{PO}_4^{3-}$  by  $\text{CO}_3^{2-}$  grouping can explain the decrease of crystallographic parameters. These structural changes are in agreement with previously reported results [25],[26].

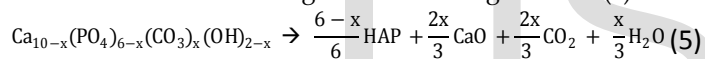
The effect of carbonate ( $\text{CO}_3^{2-}$ ) ions on the hydroxyapatite structure has been extensively studied in the literature. It is well known that carbonate has been detected as an abundant trace element with the presence of calcium and phosphorous in natural and in prepared apatite. Carbonates can be a substitute for the hydroxide ions (A-type substitution) and / or ion phosphates ( $\beta$ -type substitution). The generated materials will have a different profile of degradation and thermal stability [27],[28].

Indeed, the charge unbalance occurring when ( $\text{CO}_3^{2-}$ ) ions replace ( $\text{PO}_4^{3-}$ ) groups is primarily compensated by vacancies in Ca sites. The mechanism can be written as follows:



$\text{V}_{\text{Ca}}$  represents a vacancy on a hydroxyapatite lattice site occupied by Ca. The obtained product is hydroxyapatite with  $\beta$ -type substitution ( $\text{Ca}_{10-x}(\text{PO}_4)_{6-x}(\text{CO}_3)_x(\text{OH})_{2-x}$ ).

According to the literature [26-28],  $\beta$ -type carbonated apatite dissociates at high temperature (800 to 1050°C) into a mixture of HAP and CaO according to the following reaction (5):



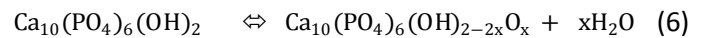
Chemical analysis performed on the calcined samples shows the presence of carbonates traces, which have not been completely removed during the thermal treatment. The chemical test confirms the absence of CaO and TGA and DTA measurements show the thermal stability of the prepared hydroxyapatite.

The result of the structural refinement shows that atom positions and distances between atoms in the prepared sample are consistent with those of the theoretical sample (Table 4), which enables us to have confidence in the refinement procedure. The perturbations in the Ca-O and P-O distance are more marked and the O-P-O angles are slightly affected. We can also notice that the B factor value is lower than 1 for Ca2, P and O2 atoms and exceeds 1 for Ca1, O1 and O3 atoms. This variation can be explained by the simultaneous insertion of carbonate and sulphate traces ions in the lattice.

Electric neutrality is ensured by reduction in the cation charge resulting from substitution of the Ca2 site by trace cations (the occupancy factors for Ca2 is lower than 1) and by the vacancy creation in the Ca1 site (the occupancy factors for Ca1 atoms exceed 1) (Table 5).

Substitutions of ion traces in HAP structure cause a decrease of volume cell and crystallographic parameters and a slight displacement of the OH atoms position. According to the literature [25],[29], such displacement can be attributed to calcium vacancies and Ca replacement by cations trace and structural changes lead to a disruption of the calcium-oxygen bonds lengths.

The decomposition during the calcinations of hydroxyapatite powder is usually promoted by the presence of impurities or the non-stoichiometry. Indeed a calcium excess ( $\text{Ca}/\text{P}>1.667$ ) results in the presence of calcium oxide (CaO), whereas a phosphorus excess ( $\text{Ca}/\text{P}<1.667$ ) results in the presence of tricalcium phosphate ( $\text{Ca}_3(\text{PO}_4)_2$ ). TGA and DTG curves presented in Fig 3 show the thermal stability of the prepared sample. The result showed weight loss between 950°C to 1300°C associated with a large endothermic effect, which is characteristic of the HAP dehydroxylation accompanied by formation of oxyapatite according to the reaction (6).



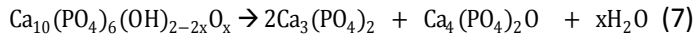
It is difficult to observe HAP transformation to oxyapatite [30], in agreement with the literature, oxyapatite is a high unstable structure which does not exist at temperatures lower than 800°C.

**Table 4:** Angles and interatomic distances with their standard deviations for prepared HAP

Angles and Interatomic distances	HAP	HAP <sub>THE</sub>
P-O(1)	1.583(9)	1.540(7)
P-O(2)	1.499(7)	1.545(8)
P-O(3)	1.549(5)	1.515(5)
O(1)-P-O(2)	110.9(9)	111.4(6)
O(1)-P-O(3)*2	111.3(7)	111.1(7)
O(2)-P-O(3)*2	108.0(5)	109.3(7)
O(3)-P-O(3)	107.2(4)	106.9(4)
Ca(1)-O(1)	2.377(5)	2.401(8)
Ca(1)-O(2)	2.458(5)	2.458(7)
Ca(1)-O(3)	2.806(7)	2.809(5)
Ca(2)-O(3)	2.327(5)	2.342(5)
Ca(2)-O(2)	2.379(7)	2.349(8)
Ca(2)-OH	2.385(4)	2.382(4)
Ca(2)-O(3)	2.493(6)	2.514(5)
Ca(2)-O(1)	2.690(8)	2.708(6)

At 1450°C, the weight loss accelerated strongly and an endothermic peak was observed indicating the oxyapatite decomposition into both tri-calcium phosphate ( $\text{Ca}_3(\text{PO}_4)_2$ )

and tetra-calcium phosphate ( $\text{Ca}_4(\text{PO}_4)_2\text{O}$ ) according to the reaction (7).



In Fig 5, decomposition of the sample and detection at 1450 °C of tri-calcium and tetra-calcium phosphate phases are confirmed by X-ray diffraction analysis.

The effects of the individual ion traces on the stability and crystallization of prepared hydroxyapatite have been studied in the literature [31],[32],[33],[34],[35]. Simultaneous insertion of one cation and one anion in hydroxyapatite lattice is also revealed and discussed, but the study of the simultaneous insertion of several cations and anions has not been studied. It is difficult to attribute the observed perturbations to a particular metal. However we can note in this study that coupled substitution of cations and anions traces at calcium and phosphor sites cause a perturbation in the P-O and Ca-O distance, the O-P-O angles are slightly affected, decrease of crystallographic parameters, decrease of volume cell and vacancies creation in Ca1 site.

The B factor value exceeds 1 for O1 and O3 atoms, which may

be due to the substitution of ion phosphor and a displacement of the position of these atoms which appears in accordance with the results of the values carried in the Table 5. This structural change leads to a slight lattice distortion ( $D_{\text{ind}} = 3.204$ ) compared to the theoretical value ( $D_{\text{ind}} = 3.079$ ). Structural rearrangements of stoichiometric hydroxyapatite in the presence of ions traces are schematized in Fig 6.

Ion traces such as  $\text{Na}^+$ ,  $\text{Mg}^{2+}$ ,  $\text{Sr}^{2+}$ ,  $\text{SO}_4^{2-}$ , and  $\text{CO}_3^{2-}$  are often detected in synthetic hydroxyapatite, even those designed for medical purposes although this does not limit their use. The limit of trace ions is not known and few studies were interested in the influence of traces ion on the physico-chemical properties of calcium hydroxyapatite [20]. We have shown in this work that coupled substitution of cations and anions trace ions with a global concentration on the order of 600 ppm affects neither the theoretical structure nor the thermal stability of the stoichiometric calcium hydroxyapatite successfully prepared from aqueous solutions under air atmosphere at room temperature and neutral pH.

**Table 5:** Atomic coordinates and equivalent isotropic displacement parameters of prepared HAP

Atom	Chem	x/a	y/b	z/c	Biso	Occ	Mult
Ca1	Ca	0.3333	0.6667	0.0016	1.1257	0.3235	4
Ca2	Ca	0.2467	0.9928	0.2500	0.9550	0.4936	6
P	P	0.3985	0.3674	0.2500	0.9204	0.4925	6
O1	O	0.3261	0.4873	0.2500	1.3958	0.5076	6
O2	O	0.5825	0.4621	0.2500	0.9660	0.5195	6
O3	O	0.3414	0.2545	0.0686	1.1253	1.0036	12
O4	O	0.0000	0.0000	0.1956	0.3020	0.1666	4
H	H	0.0000	0.0000	0.0608	1.0000	0.1666	4

**Table 6:** Atomic coordinates and equivalent isotropic displacement parameters of theoretical HAP

Atom	Chem	x/a	y/b	z/c	Biso	Occ	Mult
Ca1	Ca	0.33330	0.66670	0.00131	1.00000	0.33333	4
Ca2	Ca	0.24651	0.99311	0.25000	1.00000	0.50000	6
P	P	0.39831	0.36831	0.25000	1.00000	0.50000	6
O1	O	0.32822	0.48461	0.25000	1.00000	0.50000	6
O2	O	0.58761	0.46521	0.25000	1.00000	0.50000	6
O3	O	0.34331	0.25791	0.06933	1.00000	1.00000	12
O4	O	0.00000	0.00000	0.19787	1.00000	0.16665	4
H	H	0.00000	0.00000	0.06080	1.00000	0.16665	4

#### 4 CONCLUSION

This study reveals the structural atomic rearrangement in stoichiometric hydroxyapatite in the presence of ion traces often detected in synthetic hydroxyapatite. The sample was prepared with simple and non-polluting methods, at room temperature and neutral pH.

The coupled substitution of cation and anion trace ions, affect neither the theoretical structure nor the thermal stability of the hydroxyapatite but causes vacancies creation in both calcium and oxygen sites and a slight lattice distortion. The composition, structure and thermal stability of prepared material appears very promising for biological applications.

## REFERENCES

- [1] Herts, I.J. Bruce. *Nanomedicine (Lond)*, 2(6) (2007) 899-918.
- [2] J. Barbarand, M. Pagel. *Amer. Mineral*, 86 (2002) 473-484.
- [3] Z. L. Dong, T.J. White, B. Wei, K. Laursen. *J. Am. Ceramic. Soc*, 85 (2002) 2515-2522.
- [4] R. Z. LeGeros, P.W. Brown, B. Constanz. Boca Raton, FL, USA: CRC Press, (1994) 3-28.
- [5] O. Gauthier, J.M. Bouler, E. Aguado, R. Z. LeGeros, P. Pilet, G. Daculsi. *J. Mater. Med*, 10 (1999) 199-204.
- [6] S. V. Dorozhkin. *Materials*, 2(2) (2009)399-498.
- [7] F. Abida, Z. Hatim, A. Kheribech, M. Ellassfour, B. Elouatli, M. Jamil. *Physical and Chemical News*, 66 (2012) 84-89.
- [8] S.D. Langstaff, M. Sayer, T.J.N. Smith, S.M. Pugh, S.A.M. Hesp, W.T. Thompson. *Biomaterials*, 20 (1999) 1727-1741.
- [9] L.H. He, O.C. Standard, T.T. Huang, B.A. Latella, M.V. Swain. *Acta Biomater*, 4 (2008) 577-586.
- [10] D. Arcos, J. Rodriguez Carvajal, M. Vallet-Regi, *Chem.Mater.* 16 (2004) 2300-2308.
- [11] L. Boyer, J. Carpena, J. Lacout, *Sol. State Ionics* 95 (1997) 121-129.
- [12] X.L. Tang, X.F. Xiao, R.F. Liu, *Mater. Lett.* 59 (2005) 3841-3846.
- [13] Z. Hatim, A. Michrafy, M. Ellassfour, F. Abida. *Powder Technology*, 190 (2009) 210-214.
- [14] S. Kannan, A.F. Lemos, J.M.F. Ferreira. *Mater.*, 18 (2006) 2181-2186.
- [15] T.I. Ivanova, O.V. Frank-Kamenetskaya, A.B. Kol'tsov, V.L. Ugolkov. *Journal of Solid*, 160 (2) (2001) 340-349.
- [16] C. Liu, Y. Huang, W. Shen, J. Cui. *Biomaterials*. 22 (2001) 301-306.
- [17] L.M. Rodriguez-Lorenzo, M. Vallet-Regi. *Chem. Mater*, 12 (2000) 2460-2465.
- [18] S. Koutsopoulos. *Journal of Biomedical Materials Research Part A*, 62 (4) (2002) 600-612.
- [19] M. Jamil, F. Abida, Z.Hatim, M. Ellassfour, E. Gouri. *Mediterranean Journal of Chemistry*, 4 (1) (2015) 51-58.
- [20] L. Bernard, M. Freche, J.L. Lacout, B. Biscans. *Chemical Engineering Science*, 55 (2000) 5683-5692.
- [21] J. Rodriguez-Carvajal. *Physica B*, 192 (1993) 55-69.
- [22] K. Sudarsanan, R.A. Young. *Acta Crystallographica B*, 25 (1969) 1534- 1543.
- [23] L. J. Jha, S.M.Best, J.C.Knowles, I.Rehman, J.D.Santos and W. Bonfield, *J. Mater Sci: Mater. Med.* 8 (1997) 185 -191.
- [24] G. Montel. *Coll. Intern. CNRS*, 230 (1973) 13-18.
- [25] H. El Feki, J.M. Savariault, A. Ben Salah. *Alloys Compd*, 287 (1999) 114-120.
- [26] M. Veiderma, K. Tonsuaadu, R. Knubovets, M. Peld. *Journal of Organometallic Chemistry*, 690 (2005) 2638-2643.
- [27] J.P. Lafon, E. Champion, D. Bernache Assolant. *Journal of the European Ceramic Society*, 28 (1) (2008) 139-147.
- [28] J. C. Labarth, G. Bonel, G. Montel. *Ann. Chim*, 8 (1973) 289-301.
- [29] H. El Feki, J.M. Savariault, A. Ben Salah, M. Jemal. *Solid State Sciences* 2 (2000) 577-586.
- [30] J. C. Trombe, G. Montel. Some features of incorporation of oxygen in different oxidation states in apatite lattice I. *J Inorg Nucl Chem*, (1977) 40 : 15-21.
- [31] R.Z. LeGeros, *Apatite in biological systems*, *J. Prog. Cryst. Growth Charact.* 4 (1981) 1-45.
- [32] E. Landi, S. Sprio, M. Sandri, A. Tampieri, L. Bertinetti, G. Martra, *J. Key Eng. Mater.* 361-363 (2008) 171-174.
- [33] D. Laurencin, N. Almora-Barrios, N.H. de Leeuw, C. Gervais, C. Bonhomme, F. Mauri, W. Chrzanowski, J.C. Knowles, R.J. Newport, A. Wong, Z. Gan, M.E. Smith, *Biomaterials* 32 (2011) 1826-1837.
- [34] O. Kaygili, S.V. Dorozhkin, S. Keser, *Mater. Sci. Eng. C* 42 (2014) 78-82.
- [35] Omer Kaygili, Serhat Keser, Mustafa Kom, Yesari Eroksuz, Sergey V. Dorozhkin, Tankut Ates, Ibrahim H. Ozeran, Cengiz Tatar, Fahrettin Yakuphanoglu, *Materials Science and Engineering C* 55 (2015) 538-546.